

ON THE NONLINEAR NORMAL MODE INITIALIZATION

Hung-Chi Kuo¹

and

Jen-Her Chen²

1: Department of Atmospheric Sciences
National Taiwan University, Taipei, Taiwan, R.O.C.

2: Computer Center, Central Weather Bureau, Taipei, Taiwan, R.O.C.

1. INTRODUCTION

One would expect that improvements in numerical weather prediction will result from the integration of more "exact" models initialized with more "accurate" initial data. More accurate initial data can be obtained by better instrumentation, careful observations, data quality control and improved objective analysis and initialization. More exact models may be achieved by integrating a more correct set of equations, for dynamical as well as physical forcings (parameterization) formulations, and from the application of more accurate numerical methods to solve these equations.

Ever since the first successful integration of an atmospheric model, there has been an uninterrupted succession of improvement in dynamical model: from nondivergent barotropic equations (Charney et al. 1950) to quasi-geostrophic barotropic (Charney et al. 1956) to "filtered" baroclinic (Charney 1962) to "primitive" equations (Schuman and Hovermale 1968). Improvements in the physical parameterization due to unresolved motions have resulted in great improvement of weather forecasts, especially for longer range integrations, and of climate simulations. These include, for example, detailed boundary layer with surface hydrology and energy balance (e.g. Deardoff 1978), moist convection and cumulus parameterization (e.g. Arakawa and Schubert 1974; Kuo 1974), unresolvable scale cascade (Leigh 1971; Boer et al. 1984) and recently the development of gravity-wave drag (McFarlane 1987).

Accuracy methods reduce the truncation errors. For example, the spectral method is very accurate for the horizontal discretization due to its "exponential convergence" property. The finite element methods can be used advantageously over conventional finite differences in limited-area model (e.g. Staniforth and Daley 1977). However, the accuracy is not the whole picture for the choice of numerical methods. The need for the accuracy motivates the development of more efficient schemes. For example, the development of the semi-implicit method (Robert et al. 1972) has made possible an early operational implementation of primitive equation models. The advent of the spectral transform method (Eliassen et al. 1970) as well as the advent of Fast Fourier Transform (FFT) has made the spectral methods more attractive for practical applications. Recently the semi-Lagrangian methods (Robert

1981) has allowed a reduction in the number of timesteps required to integrate a model for a given period. The net effect of more efficient numerics is similar to that of more accurate ones in that it allows the use of more expensive, more exact numerics, higher resolution or more sophisticated physics, at the same computational cost.

In this paper, we report our efforts in the direction of more "accurate" initial data. In particular, we concentrate on the procedure of nonlinear normal mode initialization. We discuss the basis and the results of the nonlinear normal mode initialization. The nonlinear normal mode initialization will be used in the Central Weather Bureau's second generation global spectral model. Since the implementation of the nonlinear normal mode initialization require a discretized global model to produce the time tendency, we present the spectral discretized global model, the spherical harmonics basis function and the spectral transform techniques in section 2. The nonlinear normal mode initialization are discussed in section 3. Section 4 presents the test of nonlinear normal mode initialization in mid-latitude and tropics. Section 5 gives concluding remarks.

2. GOVERNING EQUATIONS AND SPECTRAL TRANSFORM TECHNIQUES

a. governing equations

The primitive equations, which are derived from the Euler equations of compressible fluid motion with hydrostatic balance and the trational approximation (Phillips, 1966), is used here. The vertical coordinate is the sigma coordinate ($\sigma = (p - p_{top}) / (\pi - p_{top})$). Here π denotes the surface pressure and p_{top} denotes the pressure (fixed) at model top. The adiabatic governing equations in the spherical geometry are

$$\frac{\partial \pi}{\partial t} = - \int_0^1 (\nabla \cdot \pi \vec{V}) d\sigma, \quad (2.1)$$

$$\pi \dot{\sigma} = - \left\{ \sigma \frac{\partial \pi}{\partial t} + \int_0^\sigma (\nabla \cdot \pi \vec{V}) d\sigma' \right\}, \quad (2.2)$$

$$\frac{\partial \Phi}{\partial P} = -c_p \theta, \quad (2.3)$$

$$\frac{\partial \zeta}{\partial t} = -\alpha(G, H), \quad (2.4)$$

$$\frac{\partial D}{\partial t} = \alpha(H, -G) - \nabla^2(\Phi + E), \quad (2.5)$$

$$\frac{\partial \theta}{\partial t} = -\frac{U}{1-\mu^2} \frac{\partial \theta}{\partial \lambda} - V \frac{\partial \theta}{\partial \mu} - (\dot{\sigma} \frac{\partial p}{\partial \sigma}) \frac{\partial \theta}{\partial p}, \quad (2.6)$$

where λ the longitude, φ the latitude, $\mu = \sin(\varphi)$, a the radius of earth, $f = 2\Omega \sin(\varphi)$ with the angular rotation rate of the earth denoted by Ω , $U = u \cos(\varphi)/a$, $V = v \cos(\varphi)/a$, $P = (p/p_0)^{R/c_p}$ and $E = \frac{1}{2}(U^2 + V^2)a^2/(1-\mu^2)$. The operator $\alpha(A, B)$ is defined as

$$\alpha(A, B) = \frac{1}{1-\mu^2} \frac{\partial A}{\partial \lambda} + \frac{\partial B}{\partial \mu}.$$

From the definition of $\alpha(A, B)$, we have

$$\zeta = \alpha(V, -U), \quad (2.7)$$

and

$$D = \alpha(U, V). \quad (2.8)$$

The inversion of U and V from known ζ and D can be mostly easily done in the spectral space. The G and H in (2.1) and (2.2) are defined as

$$G = U(\zeta + f) + (\dot{\sigma} \frac{\partial p}{\partial \sigma}) \frac{\partial V}{\partial p} + c_p \frac{1-\mu^2}{a^2} \theta \frac{\partial P}{\partial \pi} \frac{\partial \pi}{\partial \mu} \quad (2.9a)$$

and

$$H = V(\zeta + f) + (\dot{\sigma} \frac{\partial p}{\partial \sigma}) \frac{\partial U}{\partial p} + \frac{c_p \theta}{a^2} \frac{\partial P}{\pi} \frac{\partial \pi}{\partial \lambda}. \quad (2.9b)$$

The hydrostatic equation takes the form of (2.3) for the reason of discretization. Detail of vertical discretization will not given here. The Lorenz grid and energy conservation finite difference is used. Equations (2.1)–(2.8) constitutes a closed system for the dependent variables vorticity (ζ), divergence (D), three-dimensional velocities (U , V and $\dot{\sigma}$), potential temperature (θ), geopotential (Φ) and terrain pressure (π). The pressure p at each σ level is computed from equation of state.

A adiabatic prediction cycle of (2.1)–(2.8) is as follows:

- (a): U , V , ζ , D , θ and π are known.
- (b): Predict π by (2.1).
- (c): Diagnose $\dot{\sigma}$ by (2.2).
- (d): Diagnose Φ from known θ by (2.3).
- (e): Compute G , H and thus the tendencies (right hand side of (2.4)–(2.6)).
- (f): Predict ζ , D and θ by (2.4)–(2.6).
- (g): Diagnose U and V from ζ and D by (2.7) and (2.8).
- (h): Go back to step (b).

b. spectral expansions

In this section we derive the spectral representation of the field variables and discuss the nature of the corresponding Gaussian grid point value.

The spectral expansion of any global field X with a triangular truncation M is defined by

$$X(\lambda, \mu, t) = \sum_{m=-M}^M \sum_{n=|m|}^M X_n^m(t) P_n^m(\mu) e^{im\lambda}. \quad (2.10)$$

Because the global field is real, we have $X_n^m = X_n^{-m*}$, and only the spectral coefficients for nonnegative m need to be

stored (here $*$ denotes the complex conjugate). The $P_n^m(\mu)$ are the normalized associated Legendre functions of degree n and order m , defined by

$$P_n^m(\mu) = \left\{ \frac{2n+1}{2} \frac{(n-m)!}{(n+m)!} \right\}^{1/2} (1-\mu^2)^{m/2} \frac{d^m P_n(\mu)}{d\mu^m}, \quad (2.11)$$

where $P_n(\mu)$ is the ordinary Legendre polynomial given by

$$P_n(\mu) = \frac{1}{2^n n!} \frac{d^n}{d\mu^n} (\mu^2 - 1)^n. \quad (2.12)$$

With the above normalization, the orthonormality condition

$$\int_{-1}^{-1} P_n^m(\mu) P_l^m(\mu) d\mu = \delta_{nl} \quad (2.13)$$

holds. The spectral coefficients are obtained from (2.10) by applying the orthogonality property of the spherical harmonics:

$$X_n^m(t) = \frac{1}{2\pi} \int_{-1}^{+1} \int_0^{2\pi} X(\lambda, \mu, t) P_n^m(\mu) e^{-im\lambda} d\lambda d\mu. \quad (2.14)$$

The integral with respect to λ in (2.14) is performed using fast Fourier transform (FFT). The remaining integral is evaluated by a Gaussian quadrature:

$$X_n^m(t) = \sum_{j=1}^K w_j X_m(t, \mu_j) P_n^m(\mu_j) \quad (2.15)$$

where the w_j are the Gaussian weights and X_m is the Fourier transform of X . The Gaussian latitudes φ_j (μ_j) are determined as the zeros of the ordinary Legendre polynomial of order K . The Gaussian sum is exact for any polynomial of degree $2K - 1$. The weight w_j is given by

$$w_j = \int_0^\infty e^{-\mu} \prod_{i \neq j}^K \left[\frac{\mu - \mu_i}{\mu_j - \mu_i} \right] d\mu. \quad (2.16)$$

Finally we can transform the spectral coefficients to physical grid point by

$$X(\lambda_l, \mu_j, t) = \sum_{m=-M}^M \sum_{n=|m|}^M X_n^m(t) P_n^m(\mu_j) e^{im\lambda_l}. \quad (2.17)$$

Equations (2.15) and (2.17) constitutes the transform pair with (2.15) transforms a variable from physical space to spectral space while (2.17) transforms back. The precalculated X_m for (2.15) and the summation over m in (2.17) are performed by FFT's. The spectral coefficients of nonlinear terms are evaluated by the transform method. To eliminate aliasing error in the transformation of quadratic nonlinear terms, $3M + 1$ points in λ and $K = (3M + 1)/2$ points in μ are needed in the physical domain.

The Legendre functions were computed from recursion formulas recommends by Belousov (1962). The method involves values at $(m, n - 1)$, $(m - 2, n - 1)$, and $(m - 2, n - 2)$:

$$P_n^m = c_n^m P_{n-2}^{m-2} - d_n^m \sin(\varphi) P_{n-1}^{m-2} + e_n^m \sin(\varphi) P_{n-1}^m, \quad (2.18)$$

where

$$c_n^m = \left\{ \frac{(2n+1)(m+n-1)(m+n-3)}{(2n-3)(m+n)(m+n-2)} \right\}^{1/2},$$

$$d_n^m = \left\{ \frac{(2n+1)(m+n-1)(n-m+1)}{(2n-1)(m+n)(m+n-2)} \right\}^{1/2},$$

$$e_n^m = \left\{ \frac{(2n+1)(n-m)}{(2n-1)(m+n)} \right\}^{1/2}.$$

We note that this formula requires previous values in the whole triangles defined by the points $(0, 0)$, $(0, n-1)$, $(m, n-1)$ in the (m, n) wavenumber plane. Values for $m=0$ and $m=1$ must be obtained independently. The Belousov method can be implemented as

$$P_n^0 = A_n \sum_{j=0}^{(n-1)/2} b_{jn} \sin((n-2j)\varphi) + \frac{\delta_{n/2,n}}{2}$$

$$P_n^1 = A_n \sum_{j=0}^{(n-1)/2} b'_{jn} \cos((n-2j)\varphi)$$

where δ is 0 for n odd and 1 for n even. The A_n , b_{jn} and b'_{jn} are obtained from the relations

$$A_n = A_{n-1} \left\{ 1 - \frac{1}{(2n)^2} \right\}^{1/2}, \quad A_0 = \sqrt{2}$$

$$b_{j+1,n} = b_{jn} \frac{2j-1}{j} \frac{n-(j-1)}{2n-(2j-1)}, \quad b_{0n} = 1,$$

$$b'_{jn} = \frac{n-2j}{n(n+1)^{1/2}} b_{jn}.$$

From the governing equations in section 2, the grid point values of the horizontal derivatives are needed for the calculation of the time tendencies of the dependent variables. The discrete values of the horizontal derivatives are obtained from the expansion (2.10), which we used to obtain

$$\left[\frac{\partial X}{\partial \lambda} \right]_{ij}(t) = \sum_{m=-m}^M \sum_{n=|m|}^M im X_n^m(t) P_n^m(\mu_j) e^{im\lambda_i} \quad (2.19)$$

and

$$\left[\frac{\partial X}{\partial \mu} \right]_{ij}(t) = \sum_{m=-m}^M \sum_{n=|m|}^M X_n^m(t) \left[\frac{\partial P_n^m(\mu_j)}{\partial \mu} \right] e^{im\lambda_i}. \quad (2.20)$$

The evaluation of the advection tendency terms requires the computation of the grid point values of the cosine weighted velocities, U and V . By the aid of stream function, velocity potential and the relationship

$$\nabla^2 \{ P_n^m(\mu) e^{im\lambda} \} = - \left[\frac{n(n+1)}{a^2} \right] P_n^m(\mu) e^{im\lambda},$$

the U and V are related by vorticity ζ and divergence D by

$$U(\lambda, \mu, t) = \sum_{m=-m}^M \sum_{n=|m|}^M \frac{-im}{n(n+1)} D_n^m(t) P_n^m(\mu) e^{im\lambda}$$

$$+ \sum_{m=-m}^M \sum_{n=|m|}^M \frac{1-\mu^2}{n(n+1)} \zeta_n^m(t) \frac{dP_n^m(\mu)}{d\mu} e^{im\lambda}, \quad (2.21)$$

and

$$V(\lambda, \mu, t) = \sum_{m=-m}^M \sum_{n=|m|}^M \frac{-im}{n(n+1)} \zeta_n^m(t) P_n^m(\mu) e^{im\lambda}$$

$$+ \sum_{m=-m}^M \sum_{n=|m|}^M \frac{1-\mu^2}{n(n+1)} D_n^m(t) \frac{dP_n^m(\mu)}{d\mu} e^{im\lambda}. \quad (2.22)$$

The spectral coefficients of the vorticity and the divergence can be obtained from the grid point fields of U and V by using the spectral representations, which are given by (2.21) and (2.22), the orthogonality of the expansion functions, and the zero boundary conditions of U and V at the poles. The final form is written,

$$\zeta_n^m(t) = \frac{1}{2\pi} \int_0^{2\pi} \int_{-1}^1 \frac{im}{1-\mu^2} V(\lambda, \mu, t) P_n^m(\mu) e^{-im\lambda} d\mu d\lambda$$

$$+ \frac{1}{2\pi} \int_0^{2\pi} \int_{-1}^1 U(\lambda, \mu, t) \frac{dP_n^m(\mu)}{d\mu} e^{-im\lambda} d\mu d\lambda, \quad (2.23)$$

and

$$D_n^m(t) = \frac{1}{2\pi} \int_0^{2\pi} \int_{-1}^1 \frac{im}{1-\mu^2} U(\lambda, \mu, t) P_n^m(\mu) e^{-im\lambda} d\mu d\lambda$$

$$- \frac{1}{2\pi} \int_0^{2\pi} \int_{-1}^1 V(\lambda, \mu, t) \frac{dP_n^m(\mu)}{d\mu} e^{-im\lambda} d\mu d\lambda. \quad (2.24)$$

The integrals in (2.21) and (2.22) are calculated in the same manner as (2.17) while integrals in (2.23) and (2.24) are calculated the same manner as (2.15).

3. NONLINEAR NORMAL MODE INITIALIZATION

To perform *NNMI* we need expand the model variables in terms of its normal mode. This is the same as the eigenfunction expansions. The eigenvalue problem is essentially the problem of determining the dependence of the general behavior of eigenfunction on the eigenvalue and the dependence of the eigenvalue on the boundary condition imposed on the eigenfunction.

We will consider the adiabatic nonlinear normal mode initialization in our development. The basic procedure of Nonlinear Normal Mode Initialization (*NNMI*) is illustrated in terms of vertical and horizontal transforms.

a. vertical transform

The vertical transform reveals that the linearized primitive equations is equivalent to a set of the linearized shallow water equations with different equivalent depth (gravity wave speed). Using the usual notation, the unforced, nonlinear vertically discrete model prognostic equations can be written in the form

$$\frac{\partial \zeta_k}{\partial t} + 2\Omega \mu D_k + 2\Omega V_k = N_{\zeta k}, \quad (3.1a)$$

$$\frac{\partial D_k}{\partial t} - 2\Omega \mu \zeta_k + 2\Omega U_k + \nabla^2 \Phi_k = N_{Dk}, \quad (3.1b)$$

and

$$\frac{\partial \Phi_k}{\partial t} + S D_k = N_{\Phi k} \quad (3.1c)$$

where N_k are nonlinear terms, \mathbf{S} is an $L \times L$ matrix, k the vertical level index and L is the number of the vertical level used. The \mathbf{S} depends on the vertical discretization scheme and the choice of the basic state. The prognostic equations (3.1) form the foundation for the separation of the dependent variables ζ , D and Φ into horizontal and vertical structures.

The vertical transform of (3.1) involves finding the eigenvectors of \mathbf{S} and using these orthonormal eigenvectors to perform similarity transform. This will transform \mathbf{S} into a diagonal matrix with component C_k^2 , the square of gravity wave speed in k th vertical mode. After the vertical transform, we get a set of the discrete shallow water equations. The discrete shallow water system (horizontal structure equations) can be written symbolically as

$$\frac{\partial \mathbf{W}_k}{\partial t} + L_k \mathbf{W}_k = \mathbf{N}_k, \quad (3.2)$$

with the equivalent depth of C_k^2 is contained in the linear operator L_k .

Although we have started with (3.1), which has a zero basic wind state, the whole argument of vertical transform would have applied even if we had variable zonal and meridional mean winds $U(x, y, t)$ and $V(x, y, t)$ as long as they are not function of σ . Provided that the basic state temperature is a function of σ only and $\sigma_s(p_s)$ and p_s remain constant in the vertical transform.

It should be mentioned that the sufficient conditions to perform the vertical transform are that the atmosphere is hydrostatic and stable. The stable atmosphere (i.e. $d\theta/dz > 0$) guarantees the positive definiteness of C_k^2 . Since matrix \mathbf{S} comes from a Sturm-Liouville operator, the eigenvalues are of the order of k^2 and the gravity speed of each internal vertical mode is $C_k = O(1/k)$. Namely, the k th internal mode has the speed of $O(C_1/k)$ where C_1 is the gravity wave speed of the first internal mode.

b. horizontal transform

We now try to solve this discrete analog of the Sturm-Liouville problem. With the proper choice of basic state, L_k is usually a skew-Hermitian operator. Namely,

$$\langle L_k \mathbf{f}, \mathbf{g} \rangle = \langle \mathbf{f}, -L_k \mathbf{g} \rangle, \quad (3.3)$$

where $\langle \cdot, \cdot \rangle$ is a proper inner product and functions g and f satisfy boundary conditions of our system. The inner product will be the Hough transform for the global model. The skew-Hermitian operator has the following properties: the eigenvalues are imaginary, eigenfunctions are orthogonal and more importantly, eigenfunctions form a complete set. These properties can be written as

$$L_k \mathbf{K}_{kmns}(\lambda, \mu) = i\nu_{kmns} \mathbf{K}_{kmns}(\lambda, \mu), \quad (3.4)$$

where the imaginary eigenvalues $i\nu_{kmns}$ of L_k operator are the frequencies of the model's normal mode. The eigenvectors $\mathbf{K}_{kmns}(\lambda, \mu)$ are the well known Hough function on the sphere. The $\mathbf{K}_{kmns}(\lambda, \mu)$ satisfy the orthonormal condition

$$\langle \mathbf{K}_{kmns}(\lambda, \mu), \mathbf{K}_{k'm'n's'}(\lambda, \mu) \rangle = \begin{cases} 1, & \text{if } (k, m, n, s) = (k', m', n', s') \\ 0, & \text{otherwise.} \end{cases} \quad (3.5)$$

With the completeness property, we have the eigenfunction expansions for the vector \mathbf{W}_k

$$\mathbf{W}_k(t, \lambda, \mu) = \sum_{kmns} W_{kmns}(t) \mathbf{K}_{kmns}(\lambda, \mu), \quad (3.6)$$

where m, n denotes wavenumbers in the zonal and meridional directions and s the type of motions such as Rotational waves and inertial gravity waves. With orthonormal property of (3.5), we compute $W_{kmns}(t)$ by

$$W_{kmns}(t) = \langle \mathbf{W}_k(t, \lambda, \mu), \mathbf{K}_{kmns}(\lambda, \mu) \rangle. \quad (3.7)$$

Equations (3.6) and (3.7) are the transform pair of our eigenexpansions.

We now ready to derive the spectral equation of $\mathbf{W}_{kmns}(t)$ by taking the inner product of (3.3) and $\mathbf{K}_{kmns}(\lambda, \mu)$ to obtain

$$\langle \frac{\partial \mathbf{W}_k}{\partial t}, \mathbf{K}_{kmns}(\lambda, \mu) \rangle + \langle L_k \mathbf{W}_k, \mathbf{K}_{kmns}(\lambda, \mu) \rangle = \langle \mathbf{N}_k, \mathbf{K}_{kmns}(\lambda, \mu) \rangle. \quad (3.8)$$

Using the definition of skew-Hermitian operator and (3.4) we obtain

$$\begin{aligned} \langle L_k \mathbf{W}_k, \mathbf{K}_{kmns}(\lambda, \mu) \rangle &= \langle \mathbf{W}_k, L_k \mathbf{K}_{kmns}(\lambda, \mu) \rangle \\ &= \langle \mathbf{W}_k, i\nu_{kmns} \mathbf{K}_{kmns}(\lambda, \mu) \rangle = i\nu_{kmns} \langle \mathbf{W}_k, \mathbf{K}_{kmns}(\lambda, \mu) \rangle. \end{aligned} \quad (3.9)$$

Equation (3.8) then becomes

$$\frac{dW_{kmns}(t)}{dt} + i\nu_{kmns} W_{kmns}(t) = N_{kmns}, \quad (3.10)$$

where

$$N_{kmns} = \langle \mathbf{N}_k, \mathbf{K}_{kmns}(\lambda, \mu) \rangle. \quad (3.11)$$

We have now transformed our original governing equations (3.1) into the spectral equation (3.11). There are many variations on this theme. One can change from sphere to f -plane to the mid-latitude or equatorial β plane, or even to the cylindrical geometry. The Hough transforms in the sphere case is replaced by the Hermite transforms

in the equatorial β plane case, by the Fourier transforms in the mid-latitude β plane case and by Bessel transform in the cylindrical geometry case. Finally, we note that a hydrostatic system is not necessary. The method works for nonhydrostatic problems using anelastic, Boussinesq or even fully compressible equations (in the last case acoustic modes arise).

c. nonlinear normal mode initialization

When the governing equations are written in normal mode form as in (3.11) the application of the NNMI is straightforward. The first step is to divide W_{kmns} into a slow mode (low frequency) part and a fast mode (high frequency) part. For NNMI, the amplitude of the slow modes are not changed, while the amplitude of the fast modes are determined by assuming the dW_{kmns}/dt is small enough at model initial time so that (3.11) becomes

$$W_{kmns} = -\frac{i}{\nu_{kmns}} N_{kmns}, \quad s = \text{fast modes}. \quad (3.12)$$

Since N_{kmns} in (3.12) is a nonlinear function of W_{kmns} , this equation is solved by the fixed point iteration described by

$$W_{kmns}^{(r+1)} = -\frac{i}{\nu_{kmns}} N_{kmns}(W_{kmns}^{(r)}), s = \text{fast modes.} \quad (3.13)$$

where the superscript r is the iteration number.

In practice, $N_{kmns}(W_{kmns}^{(r)})$ is not computed. Instead, the time tendency of the discretized model are used in the iterations. The normal mode decomposition of the fields is carried out in terms of the spectral representation of the dependent variables. Accordingly, we obtain the spectral representations of (3.1), by expanding the dependent variables in the form

$$x_k(\lambda, \mu, t) = \sum_{m=-M}^M \sum_{n=|m|}^M x_{kn}^m(t) P_n^m(\mu) e^{im\lambda}, \quad (3.14)$$

where $x_{kn}^m(t)$ is a column vector of spherical harmonic coefficients.

4. NUMERICAL RESULTS

a. Rossby-Haurwitz wave test

The initial condition in our first experiment is a wave number 6 Rossby-Haurwitz waves from the nondivergent barotropic model. Fig.1 is an amplitude normalized harmonic dial from the wavenumber 6 of the Fourier series of surface pressure along a mid-latitude ring. For this case the model is integrated without dissipating processes except the Robert time filter. Two observations are in order. First, the lack of initialization shows in large amplitude oscillations over the 24 hours. This is not unusual and will be eliminated with the NNMI. Secondly, the phase speed of the model solution is slightly less than the analytical phase speed. This too is normal because the model solution is divergent, causing a lag relative to the nondivergent solution. The slight loss in amplitude of the model solution as compared to the nondivergent barotropic solution is due to the geostrophic adjustment during the first 24 hours.

Fig. 2 is the same as Fig. 1 except that the NNMI is performed initially. It is clear that the large amplitude oscillations disappear in the initial 24 hour. In addition, the later model path (after 24 hour) as revealed by the harmonic dial is exactly the same as what is in Fig. 1. This is the ideal situation that the NNMI filtered out the initial oscillations and not affecting the final geostrophic adjustment state.

b. the Gill's tropical test

The initial condition in our second experiment is a mass source located on the equator. We considered the calculation only of the first internal mode. The physical situation is studied analytically by Gill (1980) with the long wave approximation (i.e. $dv/dt = 0$) in a linearized shallow water model on equatorial β plane. Detail analysis of the long wave approximation on a spherical baroclinic model is discussed by Stevens et al. (1990). Fig. 3 gives the steady state of the Gill's solutions. The eastward propagation of the Kelvin waves and the westward propagation of the Rossby waves are obvious. The Kelvin waves propagated with a speed that is three times faster than the Rossby waves.

Fig. 4 give the numerical results of geopotential and wind velocity at 36 hour. No NNMI is used in this computation. Fig. 5 is the same as Fig. 4 except that the NNMI

is used initially. Although the Rossby and Kelvin signatures are existed in both calculations, the NNMI yields a solution similar to Gill's results. This suggests that NNMI is not just a trick to filtered out model's initial spurious gravity waves. The NNMI is related to the balanced dynamics of the tropical atmosphere.

5. CONCLUDING REMARKS

The formulation and the results of the nonlinear normal mode initialization NNMI of an adiabatic global spectral baroclinic model are given. This development will be used in the CWB's second generation global spectral model.

In our development, the normal mode decomposition of the fields is carried out in terms of the spectral representation of the dependent variables. Temperton (1988) have shown that the implicit NNMI schemes are equivalent to explicit NNMI, except they are formulated on the model's horizontal grid rather than in terms of normal mode coefficients. In implicit NNMI, one need to solve for Helmholtz type of equations. To solve Helmholtz equation efficiently on the sphere is still a challenge for the atmospheric modeler. On the other hand, the explicit NNMI requires the eigenvector calculation and the normal mode transform in terms of spectral discretizations. The data structure of the spectral coefficients is crucial to the successful programing. Thus, it is important to point out that the modeling strategies involved for the implicit and explicit initializations are very different.

In the mid-latitude Rossby-Haurwitz wave test, the NNMI filters out the initial spurious gravity waves while not alter later model results. The improvement of short term forecasts will provide better, more noise-free, first guess fields for use in the analysis of atmospheric data. Without NNMI, good data may be rejected as being too different from the first initial guess fields that are not noise-free. By not affecting the final geostrophic adjustment, the NNMI may have little direct effect on the forecast skill. However, the indirect role of NNMI in the data analysis is of the greatest importance.

In the tropical experiment, the NNMI produces results that are related to the balanced dynamics of the tropics. This suggests that NNMI is not just a trick to filtered out model's initial spurious gravity waves. It should not be a subject of interest only regarding NWP modeling. The NNMI is related to the balanced dynamics and the invertibility principle in the atmosphere.

REFERENCES

- Arakawa, A. and W. Schubert, 1974: Interaction of a cumulus cloud ensemble with the large-scale environment, Part I. *J. Atmos. Sci.*, **31**, 674-701.
- Belousov, S. L., 1962: Tables of Normalized Associated Legendre Polynomials. Pergamon Press.
- Boer, G. J., N. A. Mcfarlane, R. Laprise, J. D. Henderson and J.-P. Blanchet, 1984: The Canadian climate centre spectral atmospheric general circulation model. *Atmos. Ocean*, **22**, 397-429.

Charney, J. G., 1962: Integration of the primitive and balance equations. *Proc. Int. Symp. Numerical Weather Prediction*. Tokyo, Meteorol. Soc. Japan, 131-152.

Charney, J. G., R. Fjortoft and J. von Neumann, 1950: Numerical integration of the barotropic vorticity equation. *Tellus*, **2**, 237-254.

Charney, J. G., B. Gilchrist and F. Schuman, 1956: The prediction of general quasi-geostrophic motions. *J. Meteor.*, **13**, 489-499.

Deardoff, J. W., 1978: Efficient prediction of ground surface temperature and moisture, with inclusion of a layer of vegetation. *J. Geophys. Res.*, **83**, 1889-1903.

Eliassen, E., B. Machenhauer, and E. Rasmusson, 1970: On a numerical method for integration of the hydrodynamical equations with a spectral representation of the horizontal fields. Report No. 2, Institut for Teoretisk Meteorologi, Kobenhavns Universitet, 35 pp.

Hoskins, B. J. and A. J. Simmons, 1975: A multi-layer spectral model and the semi-implicit method. *Quart. J. Roy. Met. Soc.*, **101**, 637-655.

Kuo, H.-L., 1974: Further studies of the parameterization of the influence of cumulus convection on large-scale flow. *J. Atmos. Sci.*, **31**, 1232-1240.

Leith, C. E., 1971: Atmospheric predictability and two-dimensional turbulence. *J. Atmos. Sci.*, **28**, 145-161.

McFarlane, N. A., 1987: The effect of orographically excited gravity wave drag on the general circulation of the lower stratosphere and troposphere. *J. Atmos. Sci.*, **44**, 1775-1800.

Phillips, N. A., 1966: The equations of motion for a shallow rotating atmosphere and the "traditional approximation." *J. Atmos. Sci.*, **23**, 626-628.

Robert, A. J., J. Henderson, and C. Turnbull, 1972: An implicit time integration scheme for baroclinic modes of the atmosphere. *Mon. Wea. Rev.*, **100**, 329-335.

Schuman, F. G. and J. B. Hovemale, 1968: An operational six-layer primitive equation model. *J. Appl. Meteor.*, **7**, 525-547.

Simmons, A. J. and M. Jarraud, 1983: The design and performance of the new ECMWF's Workshop on Numerical Methods for Weather Prediction, Volume 2, 5-9 September 1983, 113-164.

Stevens, D. E., H.-C. Kuo, W. H. Schubert, and P. E. Ciesielski, 1990: Quasi-balanced dynamics in the tropics. *J. Atmos. Sci.*, **47**, 2262-2273.

Temperton, C., 1988: Implicit normal mode initialization. *Mon. Wea. Rev.*, **116**, 1013-1031.

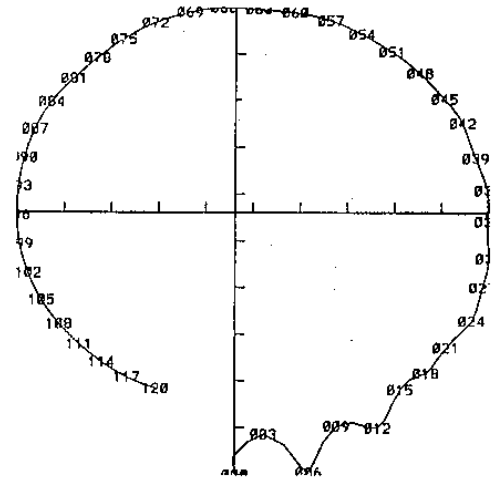


Figure 1. An amplitude normalized harmonic dial from the Rossby-Haurwitz wave test. The real and imaginary coefficients of the wavenumber 6 of the Fourier series of surface pressure along a mid-latitude ring are plotted. No NNMI is performed initially.

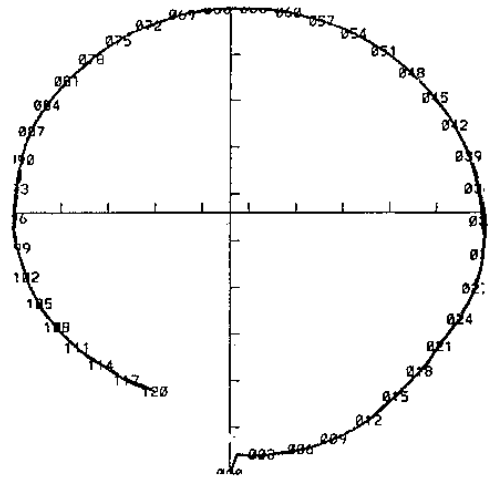


Figure 2. Same as Fig.1 except NNMI is performed initially.

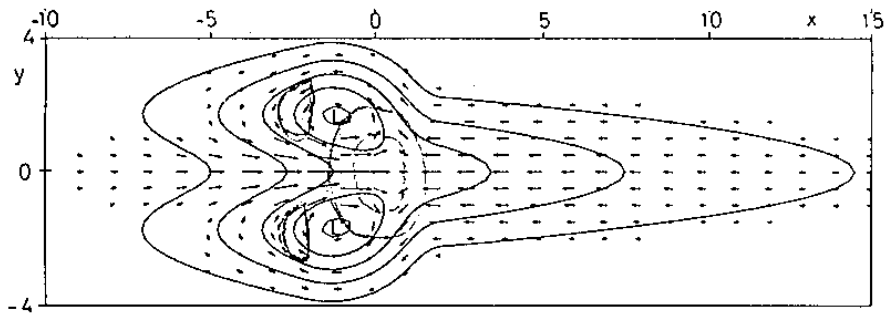


Figure 3. The steady state of the Gill's solutions. The eastward propagation of the Kelvin waves and the westward propagation of the Rossby waves are obvious. The Kelvin waves propagated with a speed that is three times faster than the Rossby waves (adapted from Gill (1980)).

GEOPOTENTIAL HEIGHT PERTURBATION AND U V AT TIME 36. (HR)

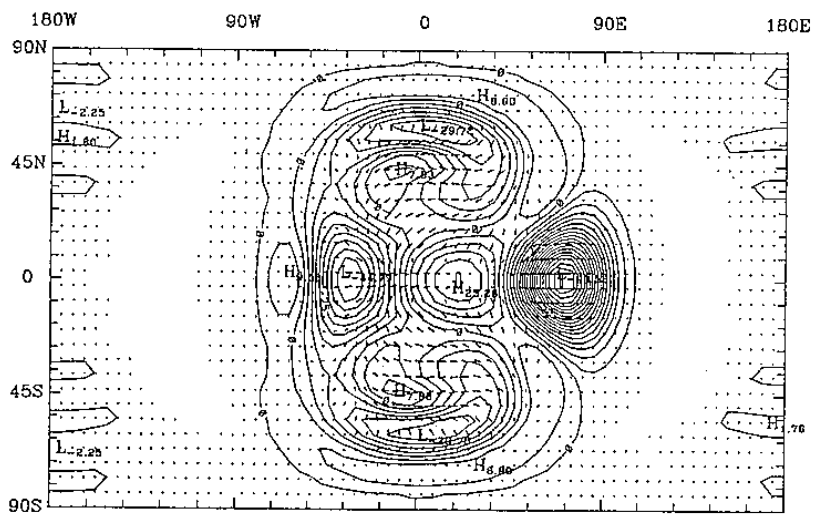


Figure 4. The numerical results of geopotential and wind velocity at 36 hour. No NNMI is used initially.

GEOPOTENTIAL HEIGHT PERTURBATION AND U V AT TIME 36. (HR)

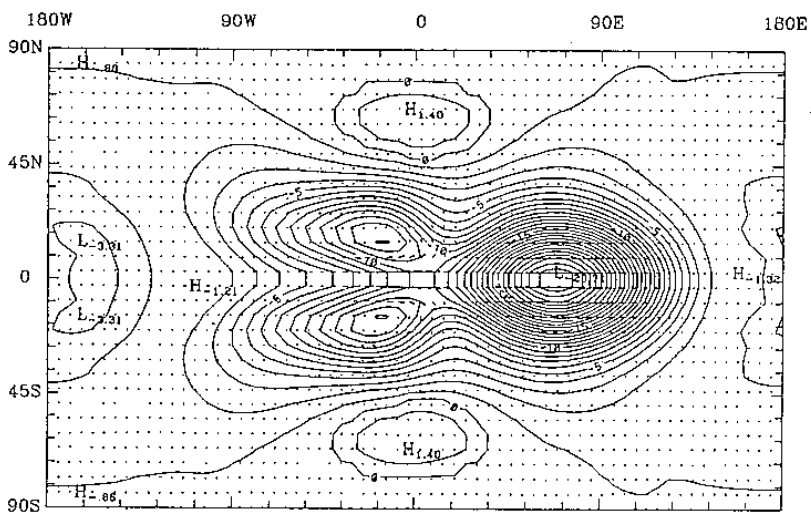


Figure 5. Same as Fig. 4 except that the NNMI is used initially.

